Development of Dual Bumper Wall Construction for Advanced Spacecraft

A. J. RICHARDSON* AND J. P. SANDERS†
North American Rockwell Space Division, Downey, Calif.

This paper describes research and development of the dual bumper wall construction for application to advanced spacecraft. Theoretical penetration mechanics were applied to size single and dual bumper test articles containing various amounts of multilayer insulation. Hypervelocity particle impact testing of candidate wall constructions was completed and the effectiveness established. The dual bumper wall was found to be over twice as efficient as the single bumper wall in resisting complete perforation, for impact velocities where projectile fragmentation occurs and where rear sheet penetration by these fragments is the major source of damage. Quantitative data are presented on the increased penetration resistance afforded by multilayer thermal insulation.

Introduction

METEOROID protection under development for advanced spacecraft has followed primarily the single bumper approach proposed by Whipple[1] who theorized that meteoroids striking a thin bumper at hypervelocity would be melted or vaporized. Therefore, the surface of a structural member spaced some distance behind the bumper need only be designed to resist impact by the particulate or vaporous debris cloud resulting from the initial impact. Early experiments[2,3] confirmed the theory showing that at impact velocities above approximately 3 km/sec even metallic particles were fragmented by a thin metallic bumper. Numerous later tests (e.g., Refs. 4–6) explored the effects of the major parameters (particle material, bumper material, and bumper spacing) on perforation resistance, with the result that this type of meteoroid protection has at this time been developed to nearly its full potential. From the standpoint of spacecraft meteoroid protection, a maximum effectiveness of approximately five is obtainable with single bumper construction, in the particle impact velocity range of 0 to 8 km/sec. Wall construction effectiveness (e) is defined as the weight per unit area of single sheet aluminum wall sized to resist perforation by a given particle, divided by the weight per unit area of the wall construction in question when sized to resist perforation of the rear sheet by the same particle.

Application of the single bumper wall construction to advanced spacecraft has been investigated by NR/SD as part of NASA funded studies of advanced planetary missions.[7,8] For the large spacecraft and long durations associated with these missions, it was found that the meteoroid protection weight penalty would range up to 3 psf of vehicle surface, and would become the over-riding structural problem. As a result, a research and development effort was initiated at NR/SD to develop lower weight meteoroid protection.[9,10] Advanced penetration mechanics[11,12] were applied which indicated that theoretically a dual bumper wall construction would have an effectiveness much greater than that provided by single bumper construction. This would be achieved by providing a first bumper sized to provide a good fragmentation and scattering of the projectile. Spaced a specific distance behind this would be a thin second bumper sized to fragment the largest debris particles from the first sheet impact. Sufficient spacing would be provided between the first and second bumper to insure that all primary debris would encounter second bumper material and be fragmented again. Behind the bumpers would be located the rear sheet, sized to resist perforation by impact of the secondary debris. This sheet would simulate either the pressure wall of a cabin module or the propellant tank wall of a propulsion module. Sufficient spacing between the second bumper and the rear sheet would be provided to allow for scattering of secondary debris, and to prevent premature destruction of the second bumper by debris reflected from the rear sheet.

Presented as Paper 71-339 at the AIAA/ASME Structures, Structural Dynamics and Materials Conference, Anaheim, Calif., April 19–21, 1971; submitted April 20, 1971; revision received December 9, 1971. This research supported by North American Rockwell Corporation.

Index categories: Meteoroid Protection Systems; Hypervelocity Impact.

* Member Technical Staff V, Structures and Mechanisms Department.

† Member Technical Staff I, Structures and Mechanisms Department.

Experimental Investigation

Testing

A test program was completed to evaluate the single and dual bumper wall configurations of Fig. 1. In each case the rear wall (t_3) represented a cabin module pressure wall or a propulsion module tank wall, and protective material was added to the outside to limit impact damage to the rear wall. Use of a nonmetallic shield (t_2) was considered in conjunction with a single bumper, and the protective effects of thermal insulation were considered in conjunction with both single and dual bumper shielding.

Test articles were designed to incorporate some of the major structural features which would be required for spacecraft application, and a typical assembled test article is shown in Fig. 2. Stringers were added to the outer bumper panels to simulate stiffening necessary for this member to resist aerodynamic boost loadings. These were fabricated with a circular opening in the center which was covered by an insert plate.

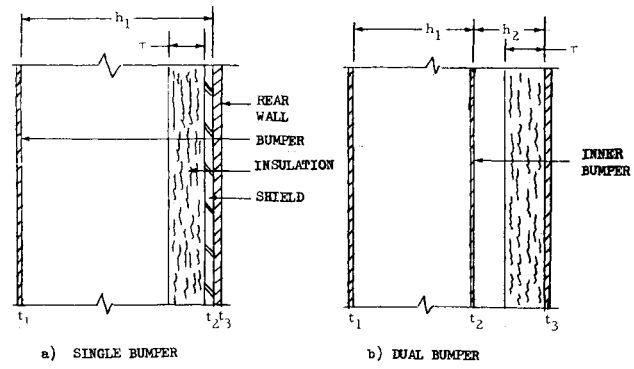

Fig. 1 Schematic target configurations.

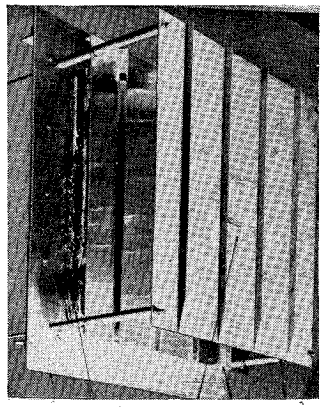

Fig. 2 Typical dual bumper test article.

Hypervelocity particles impacted on the insert plate which was changed for each test shot. Insulation blankets were of two types: 1) alternating layers of $\frac{1}{4}$ mil 1145-0 aluminum foil and 2.8 mil Dexiglass, or 2) multiple layers of $\frac{1}{4}$ mil crinkled NRC2 aluminized mylar. The measured densities were 7.2 and 1.36 lb/ft^3, respectively. Corrugations were formed in the aluminum inner bumper panels to simulate stiffening which would be required for these members to resist vibratory loadings.

To achieve the dual bumper effect, these test articles were sized nominally by the following equations. From Refs. 11 and 12

$$t_1 = 0.13 d_p \rho_p / \rho_1, \text{ cm} \quad (1)$$

$$t_2 = 0.3 t_1, \text{ cm} \quad (2)$$

$$\bar{t}_3 = 4.85 \times 10^{-5} f m_p^{0.367} \rho_p^{0.133} V_p^{2/3} / H_3^{1/4} \rho_3^{1/6}, \text{ cm} \quad (3)$$

$$h_1 = 30 d_p, \text{ cm} \quad (4)$$

$$h_2 = h_1/2, \text{ cm} \quad (5)$$

where d_p is projectile diameter (cm), ρ is density (g/cm^3), V_p is projectile velocity (cm/sec), H_3 is third sheet Brinell hardness [kg/(mm)^2], m_p is projectile mass (g), f is a finite sheet factor (1.8 for aluminum), and $\bar{t}_3$ is the minimum thickness of third sheet sufficient to resist perforation (cm). Equations (2) and (3) are based on the primary debris particles

Table 1 Test article data

Specimen no.	Specimen type	Thickness, cm				Spacing, cm		Materials[a]	
		t_1	t_2	t_3	τ	h_1	h_2	Second sheet	Insulation
1	SB	0.081	0	0.480	0	10.15	—	—	—
2	SB	0.081	0	0.480	0.63	10.15	—	—	Type 1
3	SB	0.081	0	0.480	0	30.40	—	—	—
4	SB	0.081	0.190[b]	0.318	0	9.90	—	Glass epoxy	—
5	SB	0.081	0.190[b]	0.158	0	9.90	—	Glass epoxy	—
6	SB	0.081	0.127[b]	0.318	0	9.65	—	Glass epoxy	—
7	SB	0.127	0	0.525	7.60	21.00	—	—	Type 2
8	SB	0.127	0	0.415	7.60	21.00	—	—	Type 2
9	SB	0.132	0	0.630	2.54	21.00	—	—	Type 2
10	SB	0.109	0	0.626	7.60	21.00	—	—	Type 2
11	DB	0.081	0.025	0.318	0	20.30	10.15	2014-T6	—
12	DB	0.081	0.025	0.081	0	20.30	10.15	2014-T6	—
13	DB	0.127	0.051	0.165	2.54	30.40	15.20	2024-T3	Type 2
14	DB	0.127	0.051	0.165	7.60	30.40	15.20	2024-T3	Type 2
15	DB	0.127	0.041	0.163	2.54	22.80	10.15	2024-T3	Type 2
16	DB	0.132	0.030	0.104	2.54	13.30	7.60	2024-T3	Type 2

[a] First sheet material was 2024–T3 aluminum alloy. Rear sheets were fabricated of the same alloy except for Specimen 15 which used 2014–T6.
[b] These sheets acted as shields rather than bumpers. The shield on Specimen 6 was spaced 0.318 cm away from rear sheet in an attempt to reduce rear sheet bulging.

Table 2 Hypervelocity impact data

Specimen no.	Specimen type	Projectile[a]		Rear sheet damage				Computed specimen effectiveness (e_i)
		Velocity (V_p) km/sec	Dia. (d_p) cm	Maximum penetration (p_3) cm	Bulge dia. cm	Bulge depth cm		
1	SB	6.76	0.635	0.280	—	—	Rear spall 3.48 cm dia. × 0.203 cm	3.9
2	SB	7.15	0.635	0.228	—	0.076		4.5
3	SB	7.32	0.635	0.203	—	—		4.6
4	SB	6.43	0.635	0.025	5.1	0.635		8.4
5	SB	7.00	0.635	0.025	—	—	Bulge and tear failure occurred	—
6	SB	7.32	0.635	0.102	5.1	0.940		6.8
7	SB	6.28	0.950	0.203	8.1	0.330		6.0
8	SB	6.70	0.950	0.178	11.4	0.560		6.9
9	SB	6.76	0.950	0.280	14.0	0.304		5.4
10	SB	6.68	0.950	0.076	5.1	0.228		10.3
11	DB	7.00	0.635	0.051	—	—		11.0
12	DB	6.76	0.635	0.051	—	—	Two 0.076 cm perforations	11.0
13	DB	6.45	0.950	0.033	8.9	0.228		12.2
14	DB	6.58	0.950	0.008	5.1	0.010		13.7
15	DB	6.52	0.950	0.051	15.2	0.560		12.3
16	DB	6.74	0.950	0.051	—	—	Bulge and tear failure occurred	16.1

[a] Projectile material for 0.635 cm spheres was 2024–T4 aluminum and for the 0.950 cm spheres was 2017–T4 aluminum. Test 10 used a glass projectile.

being 0.28 the diameter of the projectile and the secondary debris particles being 0.078 the diameter of projectile. Variations from the nominal sizing values were tested to determine the sensitivity of certain parameters. Test article data are presented in Table 1.

Hypervelocity impact testing was performed for NR/SD by J. Jeslis and H. Nagioka of the Illinois Institute of Technology Research Institute using the IITRI 0.60-caliber light gas gun. Test data obtained are summarized in Table 2.

Target Damage

Damage to the first sheet in each case consisted of a single hole removed by the impacting projectile. Hole diameters were nominally 0.94 cm and 1.53 cm for the 0.635 cm and 0.950 cm diameter aluminum projectiles, respectively.

Damage to the second sheet of dual bumper specimens (Fig. 3) consisted of a large hole, nominally equal to half the h_1 spacing, and several radial cracks. The material adjacent to the hole was petalled in the direction of particle travel. Individual small perforations (approximately 200) surrounded the central hole and extended nearly to the edge of the sheet.

Damage to the insulation (Fig. 4) consisted of a hole several inches in diameter through all insulation layers, with insulation melted in the vicinity of the hole. The central hole was surrounded by numerous small perforations. The insulation blankets were generally disarranged in the single bumper specimens and were held in place by the second sheet in the dual bumper specimens.

Damage to rear sheets (Figs. 5, 6 and 7) consisted of multiple small craters surrounding the central impact point, and bulging of the rear sheet material in the direction of projectile travel. In some cases, material was removed from the rear side by spallation at points opposite the larger craters, and in some cases the penetration-spall damage was sufficient to cause perforation. In some cases (tests 5 and 16), the bulging was the major damage and was sufficient to cause tearing and petalling of the rear sheet, as shown in Fig. 7.

Evaluation

Utilizing the damage data obtained, the performance of each specimen was evaluated in terms of its effectiveness as given by

$$e_i = W_a''/W_i'' \tag{6}$$

where

W_a'' = unit weight of the minimum thickness of single sheet aluminum able to resist perforation by the test projectile, g/cm^2.

W_i'' = unit weight of specimen i (including insulation) when sized to just resist perforation of the rear sheet when impacted by the test projectile, g/cm^2.

The unit weights for single sheet were computed by the expression $W_a'' = \bar{t}\rho_a$ where from Ref. 12

$$\bar{t} = 8.15 \times 10^{-4} m_p^{0.367} f \rho_p^{0.133} V_p^{2/3} / H_a^{1/4} \rho_a^{1/6}, \text{ cm} \tag{7}$$

All units are as defined for Eq. (3). The unit weight for the test articles was computed using the equation

$$W_i'' = t_1\rho_1 + \tau\rho_{in} + t_2\rho_2 + fp_3\rho_3, \text{ g/cm}^2 \tag{8}$$

where p_3 was the maximum penetration into the third sheet. Effectiveness values obtained are presented in Table 2.

Findings

The double fragmentation effect occurred in tests on the dual bumper test articles with the result that they proved to be more effective than the single bumper test articles. Typical

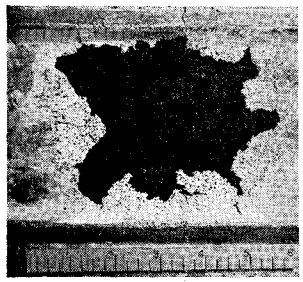

Fig. 3 Damage to inner bumper of dual bumper specimen.

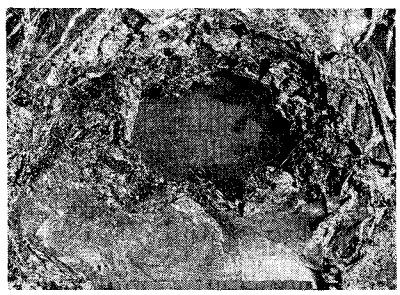

Fig. 4 Damage to multilayer insulation

Fig. 5 Cratering damage to rear sheet of a single bumper test article.

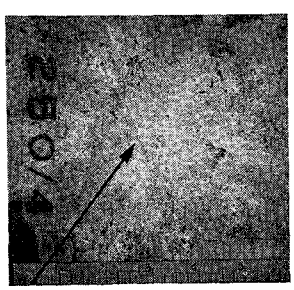

Fig. 6 Cratering damage to rear sheet of a dual bumper test article.

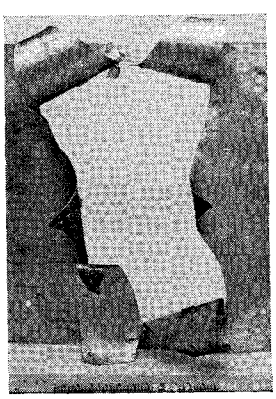

Fig. 7 Tearing damage to rear sheet of a dual bumper test article.

performance improvement is shown by comparison of data for specimen 3 with data for specimens 11 and 12 (Table 2) where effectiveness of the dual bumper specimens was found to be 160% higher than obtained with the comparable single bumper specimen.

The addition of insulation (including the low-density multilayer type) significantly increased the effectiveness of both single and dual bumper specimens. Comparison of test results from specimen 3 with those from specimen 7 shows that an effectiveness increase of 56% was obtained for single bumper specimens. Similarly, an effectiveness increase of 46% was achieved by addition of insulation to dual bumper specimens 11 and 14. (The writers have equated the effect of insulation on projectile fragments to aerodynamic drag, and corresponding theory has been successfully correlated with the data presented in this paper.)

The effectiveness of the single bumper specimens with a glass-epoxy shield located next to the aluminum rear sheets (specimens 4 and 6) was nominally 90% higher than for a comparable single bumper specimen (1). It was found that the rear sheet in this laminated configuration is more prone to tearing failure (as occurred on specimen 5) and adequate spacing should be provided to eliminate this mode of failure.

Glass projectiles are considered to be more representative of stony meteoroids in regard to fragmentation characteristics than are metallic projectiles. For comparison purposes one firing was made using a glass projectile. The effectiveness of the insulation filled single bumper test articles was found to be much higher when impacted by the glass projectile (specimen 10) than when impacted by an aluminum projectile (specimens 7 and 8).

Reduction of rear sheet penetration by use of dual bumpers can result in bulge and tear becoming the mode of rear sheet failure, as occurred on specimen 16. Here the maximum penetration was 0.051 cm into a 0.104 cm sheet and the sheet was not perforated. The sheet failed spectacularly (Fig. 7) due to bulge and tear. This mode of failure can be eliminated by adequate bumper spacing.

Conclusions

The effectiveness of the dual bumper wall construction is inherently greater than can be obtained with single bumper construction for impact velocities where projectile fragmentation occurs and where rear sheet penetration by these fragments is the major source of damage. Application of this type of meteoroid protection should be considered for spacecraft with large area-time products and/or high-reliability requirements as a means of reducing the weight of meteoroid protection.

For impact velocities where fragment damage to the rear sheet is the major source of damage, the presence of thermal insulation in a single or dual bumper spacecraft wall increases wall effectiveness and should be taken into consideration as meteoroid protection. NR/SD theory indicates that to achieve the level of improvement indicated in the tests described in this paper, the insulation must be located next to the rear sheet. Other locations would not be as beneficial.

References

[1] Whipple, F. L., "Meteoritic Phenomena and Meteorites," *Physics and Medicine of the Upper Atmospheres*, University of New Mexico Press, Albuquerque, N. Mex., 1952, pp. 137–170.

[2] Olshaker, A., "An Experimental Investigation in Lead of the Whipple 'Meteor Bumper'," *Proceedings of the Fourth Hypervelocity Impact Symposium*, Vol. 2, AIAA, New York, April 1960.

[3] Funkhauser, J. O., "A Preliminary Investigation of the Effect of Bumpers as a Means of Reducing Projectile Penetration," TN D-802, April 1961, NASA.

[4] Nysmith, C. R. and Summers, J. L., "Preliminary Investigation of Impact on Multiple-Sheet Structures and Evaluation of the Meteoroid Hazard to Space Vehicles," TN D-1039, Sept. 1961, NASA.

[5] Maiden, C. J. et al., "Thin Sheet Impact," TR 64-61, Nov. 1964, General Motors, Santa Barbara, Calif.

[6] Swift, H. F. et al., "Ballistic Limits of 6061-T6 Aluminum Bumpers Systems," TR-67-324, Oct. 1967, Air Force Materials Lab., Dayton, Ohio.

[7] Banios, E., "Study of Manned Planetary Flyby Missions Based on Saturn/Apollo Systems," SD67-549, Vol. 5, June 1967, North American Rockwell, Downey, Calif.

[8] Meston, R. D., "Technological Requirements Common to Manned Planetary Missions, NAS2-3918," SD67-621, Jan. 1968, North American Rockwell, Downey, Calif.

[9] Richardson, A. J., "Development of Advanced Wall Construction for Spacecraft Modules," STR 192, Sept. 1967, North American Rockwell, Downey, Calif.

[10] Richardson, A. J. and Sanders, J. P., "Hypervelocity Impact Testing of Multisheet Structures Containing Insulation, Cryogenic Technology IR & D Final Report CFY 1969," SD69-21, Aug. 1969, North American Rockwell, Downey, Calif.

[11] Richardson, A. J., "Formulation of Equations for Penetration Mechanics of Multisheet Structures Based on Discrete Particle Modeling," STR 177, April 1967, North American Rockwell, Downey, Calif.

[12] Richardson, A. J., "Theoretical Penetration Mechanics of Multisheet Structures Based on Discrete Particle Modeling," *Journal of Spacecraft and Rockets*, Vol. 7, No. 4, April 1970, pp. 486–489.